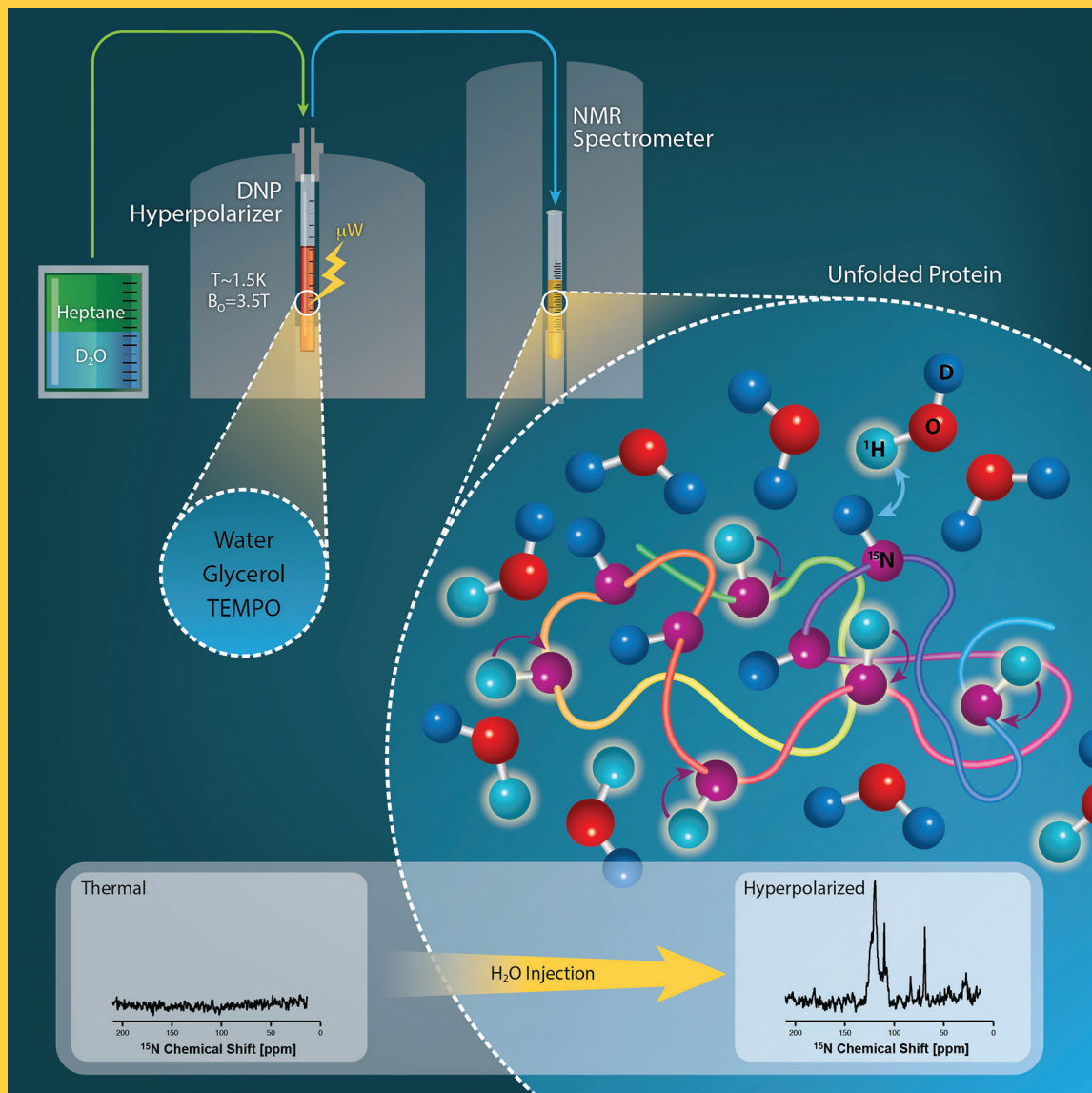


MARCH 27, 2014
VOLUME 118
NUMBER 12
pubs.acs.org/JPCB

THE JOURNAL OF PHYSICAL CHEMISTRY B

Enhancing the
Sensitivity of
Solution-Phase
Protein NMR by
Optimized Injections of
Hyperpolarized Water
(see page XA)



BIOPHYSICAL CHEMISTRY, BIOMATERIALS, LIQUIDS, AND SOFT MATTER



ACS Publications
MOST TRUSTED. MOST CITED. MOST READ.

www.acs.org

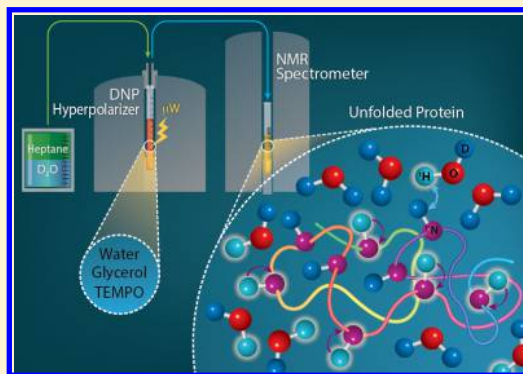
On the Potential of Hyperpolarized Water in Biomolecular NMR Studies

Talia Harris, Or Szekely, and Lucio Frydman*

Chemical Physics Department, Weizmann Institute of Science, 205 Herzl Street, Rehovot 76100, Israel

 Supporting Information

ABSTRACT: A main obstacle arising when using ex situ hyperpolarization to increase the sensitivity of biomolecular NMR is the fast relaxation that macromolecular spins undergo upon being transferred from the polarizer to the spectrometer, where their observation takes place. To cope with this limitation, the present study explores the use of hyperpolarized water as a means to enhance the sensitivity of nuclei in biomolecules. Methods to achieve proton polarizations in excess of 5% in water transferred into the NMR spectrometer were devised, as were methods enabling this polarization to last for up to 30 s. Upon dissolving amino acids and polypeptides sited at the spectrometer into such hyperpolarized water, a substantial enhancement of certain biomolecular amide and amine proton resonances was observed. This exchange-driven ^1H enhancement was further passed on to side-chain and to backbone nitrogens, owing to spontaneous one-bond Overhauser processes. ^{15}N signal enhancements >500 over 11.7 T thermal counterparts could thus be imparted in a kinetic process that enabled multiscan signal averaging. Besides potential bioanalytical uses, this approach opens interesting possibilities in the monitoring of dynamic biomolecular processes, including solvent accessibility and exchange process.



1. INTRODUCTION

Recent developments in high-field dynamic nuclear polarization (DNP), can greatly enhance the sensitivity of nuclear magnetic resonance (NMR) in solids and liquids.^{1–8} Most promising among these methods, particularly within the context of solution-phase NMR spectroscopy and imaging (MRI), is the dissolution DNP approach. Dissolution DNP improves NMR's sensitivity by executing the nuclear hyperpolarization ex situ, on a custom polarizer where the targeted sample is comixed with a stable (often organic) radical and cooled into an amorphous frozen glass.⁹ After exposing such cryogenic system to suitable microwave radiation, the very high polarization of the electron spins ($\geq 90\%$) is efficiently transferred to the surrounding nuclei in bulk. This microwave-driven polarization transfer happens over minutes or hours at $T \leq 1.5$ K; the sample is subsequently returned to the liquid state by exposing it to hot vapors, and the resulting liquid is then flushed from the polarizer into the NMR/MRI probe/coil for a rapid inductive-based detection.¹⁰ This ex situ method can create nuclear polarizations in excess of 30%,^{11–17} and for the case of small molecules, its sudden-dissolution nature can preserve much of these earnings for subsequent liquid-phase NMR observations. Such sensitivity gains can be truly outstanding, akin to years of nonstop conventional signal averaging.^{18–20} Still, when considering the use of this setup for biomolecular applications, a serious limitation arises. This derives from the short relaxation times that characterize biomolecules, particularly in the very low (<0.1 T) magnetic fields that the dissolved sample has to

negotiate between the polarizer and the spectrometer. Indeed, relaxation rates in excess of a kilohertz are typical of medium-sized biomolecules tumbling with nanosecond correlation times,^{21–23} implying that in the 1–3 s time scales that the dissolution DNP method requires for the sample to traverse through a low-field region, most of the hard-earned polarization gains will be lost. The sample hyperpolarization will be further depleted by the additional relaxation induced by the paramagnetic polarizing agent, which gets dissolved and transferred together with the targeted sample into the NMR spectrometer.

A number of alternatives have emerged over recent years to deal with this limitation. The most general among these solutions is arguably the proposal by Kockenberger et al.,²⁴ which employs a dual-magnet approach whereby the solid sample is transported from an upper DNP magnet into a lower NMR magnet, where samples are melted and observed. While also in this setup the sample transverses a low-field region in-between the magnets, it does so as a cryogenic pellet, opening an opportunity for preserving the hyperpolarization of even large biomolecules thanks to their cryogenic state. In a scheme that follows more closely the original ex situ DNP setup, Hilty and coworkers have recently described a dissolution device that maximizes sample transport speed while minimizing turbulence through a system of back-pressure regulation.^{25,26} Using this

Received: October 17, 2013

Revised: January 13, 2014

Published: January 13, 2014

system and a modified Hypersense polarizer, a total sample dissolution-to-NMR delay of 1.2 s was achieved; short enough to endow the original *ex situ* approach with 300–3000× sensitivity gains for certain ^{13}C sites in perdeuterated, unfolded polypeptides.²⁰ Yet another interesting option recently demonstrated within the context of DNP-enhanced biomolecular NMR, focuses the hyperpolarization on perdeuterated ^{15}N -labeled systems, which were allowed to slowly exchange their deuterons with protons of water acting as dissolution solvent.²⁷ Because this H/D exchange process takes place once the sample has reached the high-field NMR magnet and probe, the ^{15}N sensitivity enhancement is preserved and can be passed onward to protons.

The present study examines an alternative way to cope with these limitations, that uses hyperpolarized water as a means to enhance the sensitivity of biomolecular nuclei. We find that water protons could be spin-aligned rapidly in a cryogenic DNP setup, delivering polarizations of ~5% after their dissolution and transfer to the NMR scanner. This enhancement could be made relatively long-lived, thanks to extended relaxation times T_1 realized by gentle heating and by adding a cosolvent that executed a postmelting radical extraction. Even factoring all dilution and relaxation losses, the ensuing method led to magnetizations that were over 100× larger than thermal counterparts involving pure water placed in a high-field magnet. Upon using this hyperpolarized water to dilute a biomolecule waiting in the NMR spectrometer, a number of amine and amide groups underwent rapid exchange of their protons with H_2O , leading to a clear enhancement of their ^1H resonances. This incorporation of hyperpolarized protons also led to an Overhauser-driven heteronuclear effect, whereby ^{15}N sites that were chemically bound to solvent-exchanging protons underwent a spontaneous magnetization enhancement. ^{15}N signal enhancements equating to hundreds of times the thermal equilibrium ^{15}N polarization could thus be recorded for both backbone and sideband amide and amine sites; these effects could last over significant times, opening the possibility of exploiting them in multi-scan acquisitions. Besides enabling new bioanalytical capabilities via their sensitivity enhancements, this kind of experiment opens new opportunities to monitor dynamic biomolecular processes involving water H-exchange as reporter – including studies of protein folding and solvent accessibility.

2. MATERIALS AND METHODS

Dynamic Nuclear Polarization. Water hyperpolarization was achieved by dissolving 25 mM TEMPO radical (Sigma Aldrich, St. Louis, MO) in a 3:2 H_2O /glycerol (v/v) solution. Samples, usually of 150 μL or less, were hyperpolarized in an Oxford Instruments (Tubney Woods, Abingdon, U.K.) Hypersense 3.35 T polarizer operating at 1.5 K by irradiating a cofrozen TEMPO radical with ≤ 180 mW at ~94.1 GHz. Following DNP, samples were dissolved in 99.9% D_2O (Sigma Aldrich) and heptane (Sigma Aldrich), as specified in the text, and transferred to the NMR by a 10 bar pulse of pressurized helium gas applied over 1.5 s. ^1H dilution factors in these dissolution DNP experiments were determined by measuring the absorbance of equivalent samples containing known quantities of dissolved red food coloring; these are reported for various conditions in Table 1 of the Supporting Information. The absorbance values in the latter samples were measured on an Ultrospec 2100pro UV/visible spectrophotometer (Amersham Biosciences, Piscataway, NJ)

at a 492 nm wavelength using a 17.8 MΩ·cm H_2O sample as blank.

Sample Preparation. For the exchangeable ^1H NMR experiments (Figure 4), a concentrated sample of partially deuterated arginine was prepared by dissolving this amino acid at natural abundance and in powdered form ($\geq 98\%$ pure, Sigma Aldrich, St. Louis, MO) in 99.9% D_2O (Sigma Aldrich), adjusting the pH to ~3 with concentrated HCl, and drying it by rotary evaporation. The procedure was repeated, and the remaining powder was dissolved in 3 mL of 99% D_2O to a final concentration of 1 M. This arginine sample was inserted into the 10 mm NMR tube subsequently used in the hyperpolarized water injection experiments. For the water-derived ^{15}N enhancement experiments of small molecules (Figures 5 and 6), sample volumes and concentrations included: 500 μL of 200 mM ^{15}N -urea (Cambridge Isotopes, Cambridge, MA), 350 μL of 500 mM ^{15}N -alanine (Cambridge Isotopes), and 700 μL of 2.1 M natural abundance arginine (Sigma Aldrich) at pH ~3. All samples were prepared in 99.9% D_2O and analyzed in 10 mm NMR tubes. Finally, for the water-derived ^{15}N enhancement experiments of biomolecules (Figure 7), modified aldehyde reductase (40 kDa) was cloned into pET28_TEVH and expressed in BL21 (DE3) bacteria using 4 L of M9 minimal media supplemented with ^{15}N labeled ammonium chloride. The bacterial lysate was applied to a Ni column (HisPrep FF 16/10, GE Healthcare Biosciences, Uppsala, Sweden) and eluted with imidazole to yield a partially purified protein mix. The imidazole was removed by applying the protein mix to a preparative desalting column (HiPrep_26/10, GE Healthcare) equilibrated with phosphate-buffered saline (PBS). The protein was filtered, 0.02% NaN_3 plus Trypsin was added to it, and the mixture was subsequently incubated overnight at 37 °C to digest the reductase. The ensuing polypeptide mix was then concentrated on a Centricon with a 10 kDa molecular weight cutoff (Millipore, Billerica, MA). The flow-through contained peptides with a $M_w < 10$ kDa that were subsequently removed from a Resource column (GE Healthcare) with 90% acetonitrile and 0.1% TFA. The resulting mixture of polypeptides was frozen and lyophilized to obtain a dry powder. An ~11 mg/mL solution was prepared by dissolving the powder in 97% D_2O buffer (25 mM KH_2PO_4 , 50 mM NaCl), and its pD was adjusted to ~10 with NaOH to ensure rapid hydrogen exchange.

NMR Spectroscopy. NMR experiments were conducted in an 11.7 T Magnex magnet (Abingdon, Oxfordshire, U.K.) run by a Varian iNova console (Palo Alto, CA) and equipped with a QNP Bruker (Karlsruhe, Germany) 10 mm probe. NMR experiments were triggered upon dissolution and injection of the hyperpolarized water sample into the NMR tubes waiting with their samples inside the magnet bore. All NMR data were processed using Matlab software (The MathWorks, Natick, MA) using an exponential decay as a line-broadening function, and when needed peaks were fitted as Lorentzians using Dmfit (The Comfit Consortium, Orleans, France).²⁸

3. RESULTS

Hyperpolarizing Water. Dissolution DNP studies have shown that water samples containing 10–40 mM of a nitroxide radical mixed with the appropriate proportion of glassing agent can be efficiently polarized when irradiated by microwaves at $T \leq 1.5$ K in high magnetic fields.^{18,29,30} Figure 1 illustrates the build-up behavior for this microwave-driven water polarization, as measured by the liquid state enhancement observed after

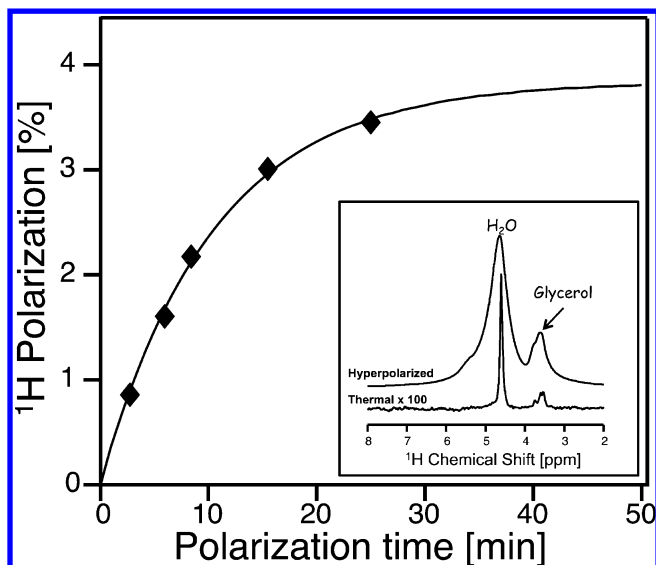


Figure 1. DNP-enhanced ^1H signal buildup observed for water as a function of the polarization time under cryogenic conditions. The experimental points arise from independent dissolution experiments, where the water signal enhancement was compared with the thermal counterpart after returning to equilibrium. Samples consisted of 30 μL of $\text{H}_2\text{O}/\text{glycerol}$ 3:2 (v/v) hyperpolarized at 1.5 K and 94.1 GHz using 25 mM TEMPO as polarizing agent and were subsequently dissolved with 3 mL of D_2O . Comparison of the resulting data to its thermal counterpart (inset) indicates a plateauing ^1H polarization under these conditions of $(3.9 \pm 0.3)\%$ and a buildup time constant of (10 ± 2) min. Alternative polarization and dissolution conditions (cf. Figure 2) can elevate the former figure beyond 5%.

dissolving a sample polarized in a 3.35T Hypersense, with 3 mL D_2O . This curve evidence a 10 ± 2 min characteristic buildup time for the solid-state polarization; in terms of the achievable postdissolution enhancement, such optimized hyperpolariza-

tion conditions led to signals decaying by ≈ 1000 -fold as they reach thermal equilibrium in the 11.7 T NMR used in this study (Figure 1, inset).

Although very promising, such enhancement figures are deceptively high. Comparisons between a hyperpolarized and a thermal signal measure relative enhancements but ignore the ^1H signal reduction due to the dilution of the hyperpolarized water with the glassing agent needed for an effective cryogenic DNP process, or the substantial dilution with nonpolarized solvent that the hyperpolarized sample undergoes upon melting and flushing it across the two magnets. To address the first of these concerns, we used glycerol as water's coglassing agent. Glycerol was chosen over other possible cosolvents, given this compound's relatively high concentration of exchangeable protons. These will be polarized as well by the solid DNP process and eventually contribute to the pool of exchangeable protons whose hyperpolarization one aims to transfer to the biomolecule. At a 3:2 water/glycerol v/v ratio, the ensuing sample polarized efficiently and still delivered $\sim 76\%$ of the exchangeable protons expected from a pure water counterpart. To address the second concern, we attempted to decrease the dilution factor by increasing the volume of hyperpolarized sample without a concomitant increase in the volume of the dissolution solvent. While the water's dilution could be reduced by a factor of ~ 10 in this fashion, this came at the cost of severely reducing the T_1 of the hyperpolarized water. This penalty reflects the fact that all efforts aimed at reducing a pellet's dilution will de facto increase the nitroxide's postdissolution concentration; because this radical efficiently polarizes the protons but is also an effective water T_1 relaxation agent, particularly in the low magnetic fields experienced by H_2O during its transfer from the polarizer to the NMR magnet,^{31,32} the net hyperpolarization achievable from these reduced-volume solutions actually drops. To reduce water's post-DNP dilution without decreasing the T_1 of the hyperpolarized ^1H , a number of alternatives were tested. The most

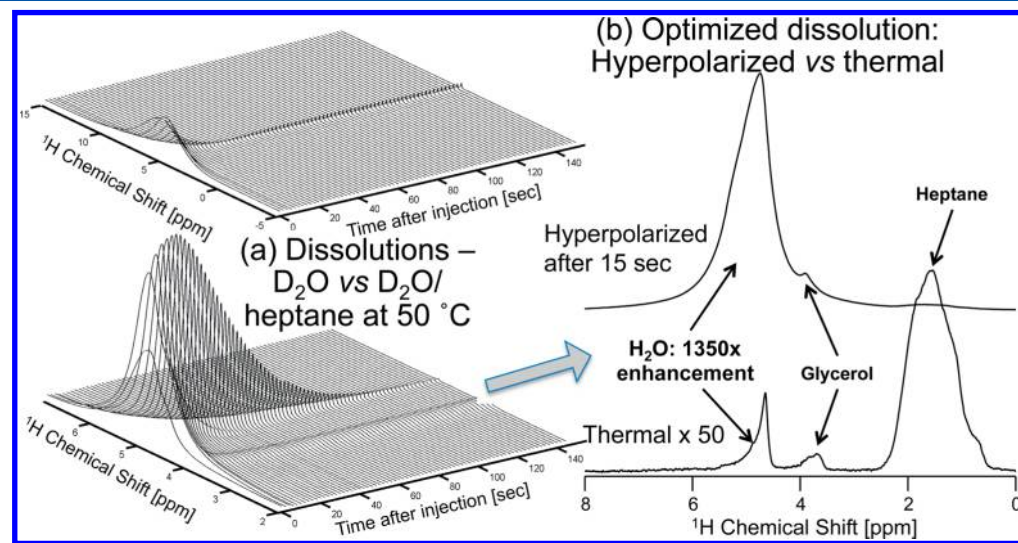


Figure 2. Improving water's hyperpolarized signal by codissolution with heptane. (a) Water signal evolution following hyperpolarization of a 150 μL 3:2 (v/v) mixture of $\text{H}_2\text{O}/\text{glycerol}$ with 25 mM TEMPO and dissolution in either 3 mL at ~ 35 $^\circ\text{C}$ D_2O (top) or in a mixture of 1.5 mL of D_2O and 3 mL of heptane with transport and measurement at ca. 50 $^\circ\text{C}$ (bottom). The relaxation time T_1 of the water resonance is extended from 3.6 (top) to 18.2 s (bottom), and the absolute enhancement at $t = 0$ is increased by a factor of 4.5. (b) Comparison between the hyperpolarized 1D ^1H NMR arising from the $\text{D}_2\text{O}/\text{heptane}$ dissolution 15 s after it has reached the NMR magnet and a thermal spectrum of the same sample. All spectra were obtained by acquiring 28 k complex data points using a small ($\sim 1^\circ$) flip-angle pulse excitation and a carrier frequency set to 2.9 ppm; time zero corresponds to the conclusion of the sample flushing from the DNP polarizer.

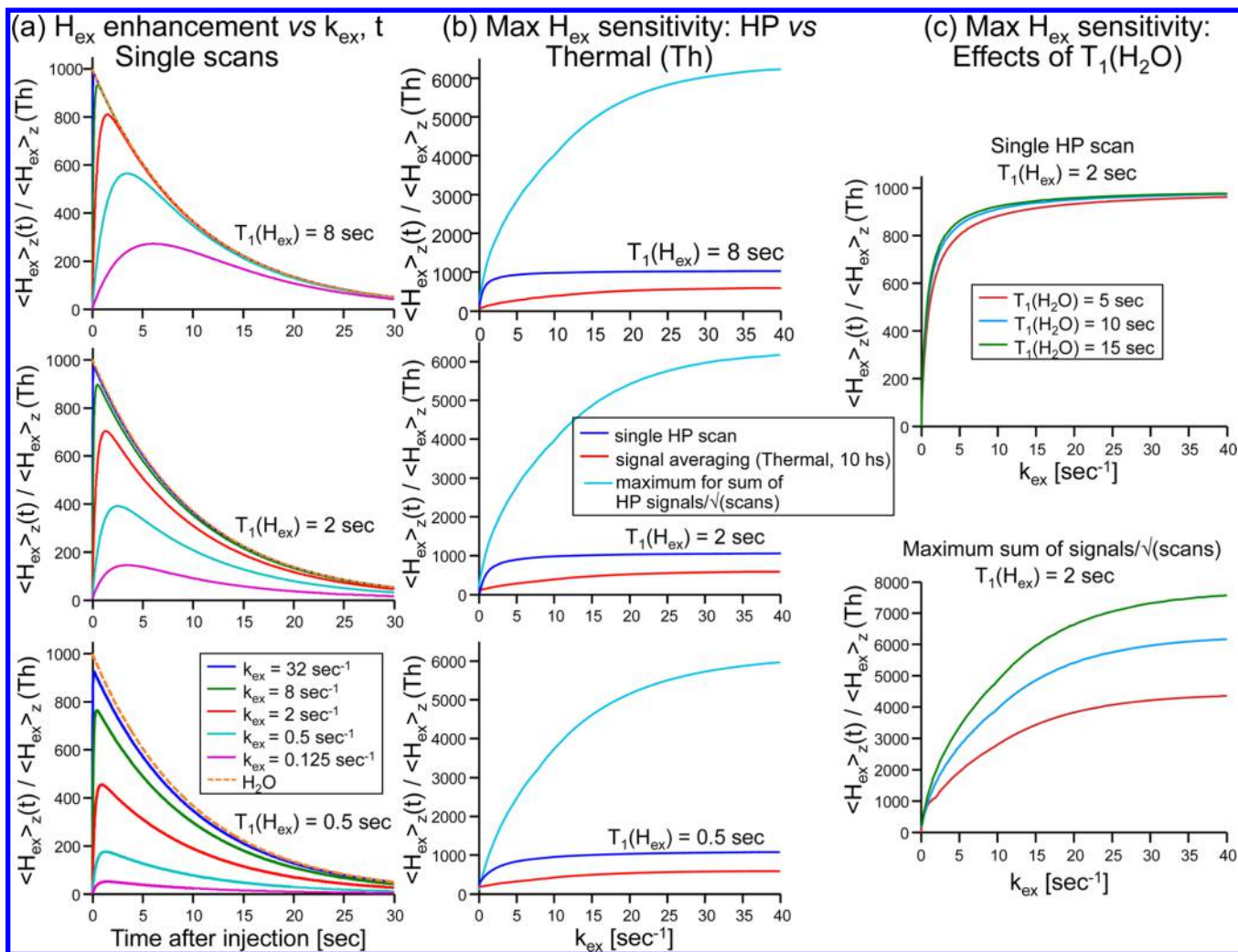


Figure 3. Calculations of the relative ^1H magnetization enhancements of protons H_{ex} due to exchange with hyperpolarized water protons. Unless otherwise stated, the relaxation of water was kept constant at $T_1^{\text{H}_2\text{O}} = 10$ s, and the initial relative enhancement of water was $\langle \text{H}_2\text{O} \rangle_z(0) / \langle \text{H}_2\text{O} \rangle_z(\text{Th}) = 1000$. (a) Enhancement as a function of time since the hyperpolarized (HP) water injection for the different exchange rate (k_{ex}) values indicated in the bottom panel. Calculations are given for three different values of $T_1(\text{H}_{\text{ex}})$ (top, middle, and bottom panels); the dashed orange line in all panels represents the decay of the water polarization with time. (b) Enhancement achievable by H_{ex} as a function of k_{ex} calculated assuming that: a single scan was measured by a 90° pulse at an optimal time after injection of hyperpolarized water (blue lines), that thermal signal averaging was performed over the course of 10 h with optimal conditions (i.e., with 90° pulses and recycle delays given by k_{ex} and not solely by $T_1(\text{H}_{\text{ex}})$; red lines), or that multiple hyperpolarized scans were done on H_{ex} at optimum times assuming minimal TR of 100 ms (cyan lines; in this latter case, we display the sum of signals collected with 90° pulses divided by square root of the number of scans). Other parameters are the same as in panel a. (c) The effect of $T_1(\text{H}_2\text{O})$ on the H_{ex} enhancement, shown for an optimized single scan acquisition (top), or for multiple scans seeking maximum SNR as a function of k_{ex} . $T_1(\text{H}_{\text{ex}}) = 2$ s, and the $T_1(\text{H}_2\text{O})$ is varied –5, 10, and 15 s (red, cyan, and green lines, respectively).

efficient among these ended up being the combined use of immiscible organic and aqueous solvents to melt and transfer the hyperpolarized water pellet.³⁰ This method reduces the dilution factor because of the phase separation that the immiscible organic solvent will undergo after the sample is transferred, as it settles outside the NMR observation coil region. At the same time, a suitable organic phase can efficiently extract the organic copolarizing TEMPO radical over the course of the sample-transfer process, thereby decreasing the aqueous phase relaxivity. Heptane was found as a useful cosolvent for achieving these dual goals without introducing substantial susceptibility-derived distortions in the ensuing lineshapes. Typically, 150 μL of hyperpolarized water samples were thus dissolved and transferred with a 1.5/3 mL mix of water/heptane, leading to a net dilution factor of ~ 8 . Further

reductions in the aqueous' phase dissolution volumes did not significantly reduce the hyperpolarized pellet's dilution factor.

Given the importance of maximizing T_1 values for the sake of minimizing polarization losses in the case of fast-relaxing nuclei like ^1H , two additional provisions were adopted. First, in all of our experiments, D_2O was used as the aqueous dissolution phase; by relying on this deuterated solvent, a ca. 4-fold increase in the T_1 of the hyperpolarized water protons was observed. In addition, the tube transferring the dissolved hyperpolarized water between the DNP and the NMR magnets as well as the NMR probe itself were preheated to ca. 40–50 $^\circ\text{C}$; this leads to an additional lengthening of the hyperpolarized ^1H 's lifetimes. Numerous other precautions were assessed in the hope of further increasing the protons' T_1 values, including the surrounding of the transfer line with ~ 1000 G magnets along its ca. 2 m route and solvent degassing,

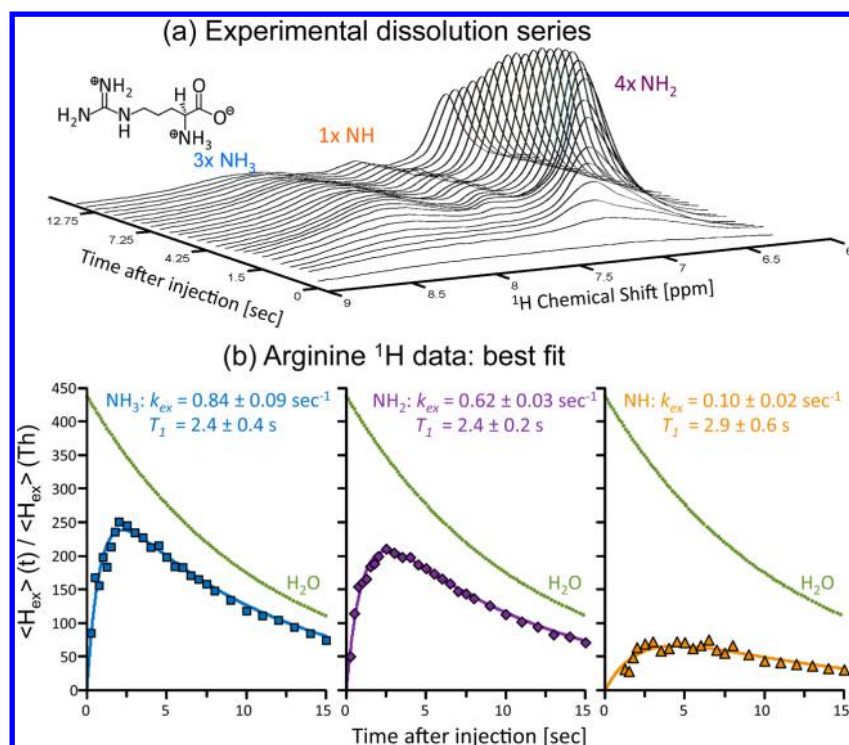


Figure 4. Transferring water hyperpolarization to the resonance of arginine's exchangeable protons. (a) Progression of arginine's ^1H NMR spectrum upon sudden dissolution of hyperpolarized water into 3 mL of a 1 M arginine sample ($\text{pD} \sim 3$) dissolved in D_2O and waiting in the 500 MHz spectrometer used to collect the data. Each trace involved the acquisition of 4k complex points, arising from a small flip-angle ($\sim 1^\circ$) excitation (carrier at 7.3 ppm) with a 0.25 s TR. The different types of protons in the arginine sample (inset: molecular formula) are indicated above their corresponding peaks. (b) Peak intensities arising from the experimental time course, together with fits to eq 2 for each arginine site (solid lines), lead to the indicated relaxation times T_1 and exchange rates k_{ex} . These fits revealed an initial water polarization enhancement of $(438 \pm 3) \times$ and a characteristic decay $T_1(\text{H}_2\text{O})$ of 10.9 ± 0.1 s; the ensuing decay curve is presented in the Figure as green dots.

yet these lead to negligible enhancements, and their use was thus discontinued. Table 1 in the Supporting Information gives further quantitative data on how each of the processes described in this paragraph assisted in achieving an enhanced water hyperpolarization at the NMR probe position.

The outcome of these efforts is summarized by the postdissolution traces in Figure 2. This compares results obtained for a dissolution employing solely D_2O , with those stemming from a joint $\text{D}_2\text{O}/\text{heptane}$ dissolution mix incorporating heating of the transfer line. The stronger, longer-lasting enhancements afforded by all aforementioned steps are clearly evidenced; unfortunately, so are the significant radiation damping effects that highly polarized water at these fields and concentrations are bound to lead to. These are reflected in both severe shifts and broadenings immediately upon dissolution, which decay as the hyperpolarization dies down. Still, judging by the areas of these small pulse-angle ($<1^\circ$) experiments, optimal cases led to a polarization $\geq 5.2\%$ and a $T_1 \geq 18$ s. When contemplating the use of such polarization as a source for enhancing the sensitivity of additional molecules, this performance should be further scaled by a $\sim 1/8$ dilution factor associated with the sample's dissolution and a 0.76 factor reflecting the decrease in labile protons owing to the use of the glycerol. All these factors combined still lead to a $\geq 120\times$ enhancement over the polarization that is present in a pure water tube polarized in a 1 GHz NMR spectrometer; this is not an insignificant gain, that compares favorably to absolute ^1H water enhancements of $\sim 15\times$ obtained at 4.7 T by conventional dissolution DNP,²⁹

and of approximately $-10\times$ obtained at 1.5 T by liquid state continuous-flow DNP.³³

Sensitivity Enhancement of Exchangeable Protons in Small Biomolecules. With these gains at hand, the use of DNP-enhanced water protons toward the magnification of NMR signals arising from labile biomolecular protons was explored. To this end, we targeted protons possessing solvent exchange rates k_{ex} that are sufficiently slow in the NMR time scale to give distinct peaks in the ensuing ^1H spectrum, and at the same time sufficiently fast to accommodate significant gains for the above-mentioned hyperpolarized water T_1 times. Because the ultimate goal is to exploit these exchange processes in biomolecules with significantly shorter T_1 values than those of the hyperpolarized water, the investigated paradigm explored the gains in polarization achieved by biomolecules that were waiting in the NMR magnet/probe and exchanged their labile protons with those of water that was suddenly injected following dissolution DNP. This approach would have the advantage that during the transfer process the polarization will decay with the longer T_1 of the water protons, and significant polarizations could be imparted even on species with short proton T_1 values. To investigate under what conditions this approach would be beneficial, basic calculations were performed on the extent by which protons H_{ex} that are initially thermally polarized will enhance their z -magnetizations $\langle \text{H}_{\text{ex}} \rangle_z$ by chemical exchange with hyperpolarized water. Assuming that the injected water hyperpolarization is much higher than its thermal (Th) counterpart (i.e., that $\langle \text{H}_2\text{O} \rangle_z(0) \gg \langle \text{H}_2\text{O} \rangle_z(\text{Th})$) and that $[\text{H}_2\text{O}] \gg [\text{H}_{\text{ex}}]$, these calculations

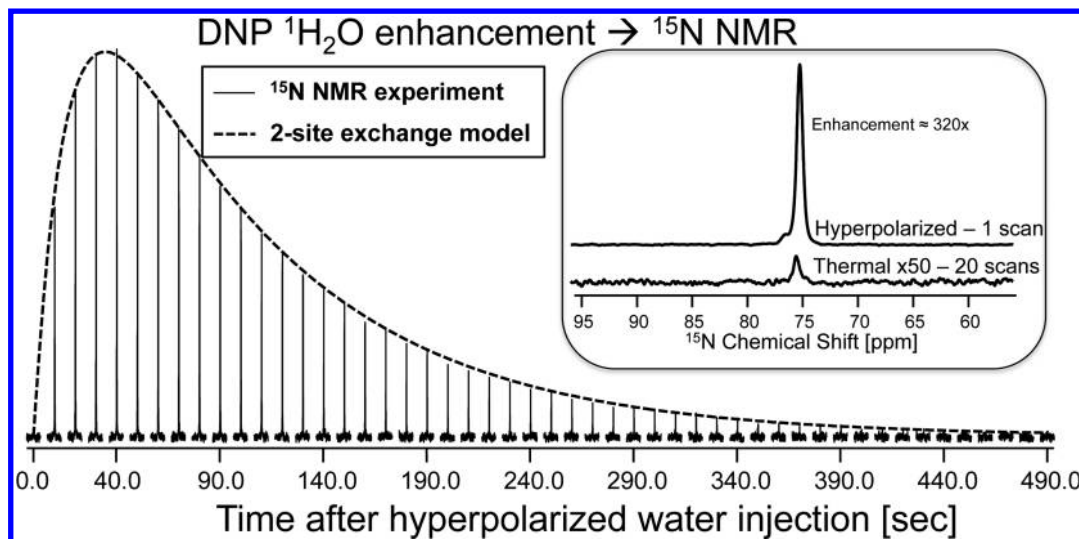


Figure 5. ^{15}N NMR enhancement achieved in ^{15}N -urea via heteronuclear polarization transfer from hyperpolarized water. Spectra were collected using a small flip-angle (9°) single-pulse irradiating on the ^{15}N channel at 76 ppm and acquiring 9 k data points (4 s acquisition time). The dashed line is a fit to the two-site exchange model in eq 3. The inset compares a single-scan DNP-enhanced ^{15}N spectrum collected using a 90° pulse applied at an optimal postinjection delay of ~ 40 s against a thermal equilibrium ^{15}N NMR spectrum measured for the same sample by signal averaging 20 fully relaxed scans over a total of 13:50 h. All measurements were done at 50°C .

follow from modified Bloch-McConnell equations³⁴ and predict a time-dependent exchangeable proton magnetization:

$$\langle H_{\text{ex}} \rangle_z(t) \approx \langle H_2\text{O} \rangle_z(0) \cdot \frac{k_{\text{ex}}}{\left(k_{\text{ex}} + \frac{1}{T_1^{H_{\text{ex}}}} - \frac{1}{T_1^{H_2\text{O}}} \right)} \cdot e^{-t/T_1^{H_2\text{O}}} \left(1 - \exp \left(- \left(k_{\text{ex}} + \frac{1}{T_1^{H_{\text{ex}}}} - \frac{1}{T_1^{H_2\text{O}}} \right) \cdot t \right) \right) \quad (1)$$

where the T_1 denotes the spin-lattice relaxation delay of the species and k_{ex} is their mutual exchange rate.

Plots of this equation for a variety of conditions are given in Figure 3a. These show that the maximum magnetization achievable by the exchangeable protons will be relatively insensitive to $T_1^{H_{\text{ex}}}$, or even to the water T_1 , but will be sensitive to the $T_1^{H_{\text{ex}}} \cdot k_{\text{ex}}$ product. Importantly, not only can high levels of single-shot polarization be achieved in this manner for H_{ex} relative to the polarization arriving with the water protons, but by applying selective pulses on the exchangeable proton sites, the water polarization can be preserved and multiple scans with enhanced signal can be acquired from a single dissolution. For a 90° selective pulsing taking place at a constant repetition time TR , the polarization contributions to the exchangeable proton signals will be described by

$$\langle H_{\text{ex}} \rangle_z(t, TR) \approx \langle H_2\text{O} \rangle_z(0) \cdot \frac{k_{\text{ex}}}{\left(k_{\text{ex}} + \frac{1}{T_1^{H_{\text{ex}}}} - \frac{1}{T_1^{H_2\text{O}}} \right)} \cdot e^{-t/T_1^{H_2\text{O}}} \left(1 - \exp \left(- \left(k_{\text{ex}} + \frac{1}{T_1^{H_{\text{ex}}}} - \frac{1}{T_1^{H_2\text{O}}} \right) \cdot TR \right) \right) \quad (2)$$

As shown in Figure 3b for a variety of instances, substantial sensitivity increases can then be obtained for the exchangeable protons. This can also be important if attempting to acquire multidimensional spectra or to follow a dynamic process. It follows as well from the last expression that although an increase in the water T_1 leads to only a slight increase in the

initial H_{ex} magnetization, the achievable polarization enhancement of the exchangeable sites in a multiscan experiment can be significantly increased by prolonging $T_1^{H_2\text{O}}$ (Figure 3c).

With these expectations as background, Figure 4 illustrates the gains that this procedure afforded when applied to arginine a small molecule possessing multiple exchanging sites. This compound exhibits different $\text{H}_2\text{O} \leftrightarrow \text{HN}^-$ exchange rates k_{ex} for the non-equivalent NH_1 , NH_2 , and NH_3 groups in the molecule, with strong pH and temperature dependencies.^{35,36} The polarization buildup is thus different for each group but is in all cases significant. A train of acquisitions following a water-based dissolution DNP experiment allows one to obtain insight into the rates of hydrogen exchange of these sites with the solvent (Figure 4a,b).

Heteronuclei Signal Enhancement. Interestingly, not only can exchangeable protons be polarized but also heteronuclei directly bound to such exchangeable protons are *spontaneously* polarized by injection of hyperpolarized water. This is illustrated in Figure 5a, which demonstrates how polarization from DNP-enhanced water ^1H migrates to urea's ^{15}N without the need for any ^1H pulsing. A train of low flip angle pulses on the ^{15}N channel evidences the slow buildup of urea's ^{15}N polarization, reaching a maximum at ~ 40 s. The decay of this polarization is also slow, reflecting a $T_1^{15}\text{N}$ that for urea in a partially deuterated solution like the one arising in this case is on the order of minutes. A number of factors are involved in this buildup/decay function, including the rate of amide/water ^1H exchange k_{ex} , the rate of $^1\text{H}-^{15}\text{N}$ cross-relaxation k_{NOE} driving the heteronuclear polarization transfer within urea, and the rates of polarization decay given by the ^1H T_1 values of the water and urea sites as well as by the ^{15}N 's own T_1 . Three-site exchange simulations (Supporting Information) show that the magnitude of the ^{15}N enhancement will depend in a complex fashion on these multiple factors. Still, fits of the experimental data based on this model reveal that the heteronuclear Overhauser transfer k_{NOE} is the rate-determining step of this $^1\text{H}_{\text{water}} \xrightarrow{k_{\text{ex}}} ^1\text{H}_{\text{ex}} \xrightarrow{k_{\text{NOE}}} ^{15}\text{N}$ polarization transfer process. With this knowledge at hand, one can propose a

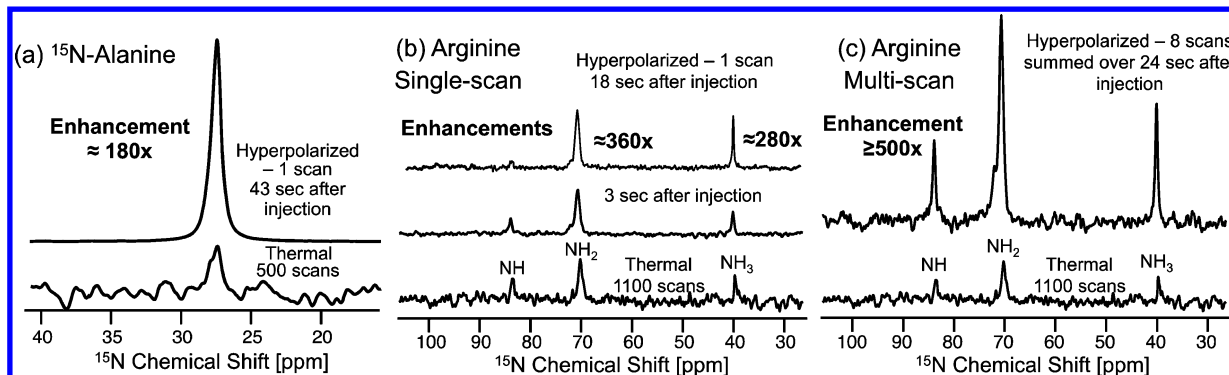


Figure 6. Enhancement vis-à-vis thermal counterparts of the ^{15}N signals of ^{15}N -alanine (a) and of natural abundance arginine (b,c) by polarization transfers from hyperpolarized water. The optimal delay in each case was extracted from simulations of the kind given in Figure 5. Hyperpolarized ^{15}N NMR spectra in panels a and b were detected in single-scan experiments using a 90° ^{15}N pulse, applied 43 and 18 s after the injection of the water, respectively. Thermal acquisitions took ca. (a) 2 and (b,c) 14 h, respectively. (c) Sum of the first eight scans collected after injection of hyperpolarized water to an arginine sample, over a total time of 24 s. An effective average enhancement $\geq 500\times$ is observed. All measurements were done at $\sim 50^\circ\text{C}$ under conditions akin to those in Figure 5. Notice that the NH of arginine has significantly lower enhancement than the other two peaks due to its slow k_{ex} at pH ~ 3 .

simpler two-site model whereby the observable ^{15}N magnetization only arises from a ^1H reservoir made available by the DNP experiment. Because this is left unperturbed apart from its relaxation back to equilibrium, the ^{15}N polarization's time evolution can be described by:³⁷

$$\frac{d}{dt} \begin{bmatrix} \langle H_z \rangle(t) \\ \langle N_z \rangle(t) \end{bmatrix} = \begin{bmatrix} -\frac{1}{T_1^H} & 0 \\ k_{^1\text{H} \rightarrow ^{15}\text{N}} & -\frac{1}{T_1^{N,\text{eff}}} \end{bmatrix} \begin{bmatrix} \langle H_z \rangle(t) \\ \langle N_z \rangle(t) \end{bmatrix} \quad (3)$$

where $k_{^1\text{H} \rightarrow ^{15}\text{N}}$ summarizes the average effects of the $\text{H}_2\text{O} \rightarrow ^{15}\text{N}$ process and $T_1^{N,\text{eff}}$ is a decay time factoring both the natural T_1 of the ^{15}N as well as the depleting effects of the pulses used to interrogate the signal.

The enveloping line in Figure 5 shows a fit of this simplified model to traces arising from this kind of experiment, leading to an effective rate $k_{^1\text{H} \rightarrow ^{15}\text{N}} = 0.29 \pm 0.02 \text{ s}^{-1}$ and times $T_1^{N,\text{eff}} \approx 89.2 \text{ s}$ and $T_1^H \approx 16 \text{ s}$. By setting $d/dt[\langle N_z \rangle(t)]_{t=t_{\text{max}}}$ to zero, this model also lets us find the approximate time leading to the maximal ^{15}N enhancement: $t_{\text{max}} = 34 \text{ s}$. For an initial degree of maximal ^1H polarization injected in the reservoir, the solution of eq 3 also predicts a maximum achievable ^{15}N polarization that from the parameters fitted in Figure 5 should be $\sim 344\times$, close to the experimentally observed value of $320\times$ (Figure 5, inset).

Figure 6 illustrates an application of this strategy to the enhancement of ^{15}N sites in alanine and arginine. For alanine, a similar analysis as the one just described suggests a maximal ^{15}N sensitivity enhancement ca. 40 s after sample injection, although with a polarization enhancement of $\sim 180\times$. A similar experiment on a 2.1 M D_2O solution of natural abundance arginine at $\text{pD} \approx 3$ shows a maximum enhancement at $\sim 20 \text{ s}$, with the $^{15}\text{NH}_2$ and $^{15}\text{NH}_3$ sites showing $\sim 360\times$ and $\sim 280\times$ levels of enhancement, respectively. Much lower enhancements ($\sim 50\times$) are observed for the NH site due to its slower rate of hydrogen exchange. It is noteworthy that because the hydrogen exchange with water for the former two arginine sites is fairly rapid, it is not necessary to wait a relatively long T_1 delay to obtain the optimum enhancement: multiple scans collected at times $\sim (k_{\text{ex}})^{-1}$ lead to significantly enhanced signals that can be averaged over several repeated scans (Figure 6c). A similar

approach could prove to be useful in the acquisition of Hadamard-encoded or sparsely sampled 2D NMR spectra.

To investigate whether these initial observations can be extended to larger biomolecules, we applied the heteronuclear transfer experiment on a lysate of ^{15}N -labeled aldehyde reductase. Trypsin-based lysis reduced the original 40 kDa M_w of this well-folded protein into an array of peptides of mostly $M_w \approx 3 \text{ kDa}$, with some 5% reaching up to the 10 kDa molecular weight cutoff used. It can be assumed that the peptides in this mixture do not contain residual structure and that their chains are fully extended. These conditions should favor a rapid exchange of their amine and amide NHs with the hyperpolarized water protons. To examine what kind of effective ^{15}N signal enhancement this could lead to, we collected a series of ^{15}N NMR spectra using 90° excitation pulses following the injection of hyperpolarized water. These results are shown in Figure 7a and confirm a sensitivity enhancement of both backbone amide and side-chain amine resonances. The build-up of these signals is relatively rapid, as expected for the high k_{ex} rates characterizing these unfolded peptides. The apparent decay of the signal enhancement by contrast, $20 \pm 1 \text{ s}$, is much slower than the overall relaxation of the backbone amides, whose global T_1^N is $1.8 \pm 0.8 \text{ s}$. This relatively slow decay reflects the T_1 of the hyperpolarized water protons, which supports the ^{15}N repolarization process between consecutive ^{15}N scans. These long lifetimes allow one to achieve an ^{15}N enhancement beyond what would be possible with a single acquisition; comparing a sum of scans collected over a 25 s period (Figure 7b, upper trace) against a thermal equilibrium ^{15}N spectrum (Figure 7b, middle trace) indicates that most peaks in the amide backbone region can be enhanced in this multiscan fashion by $>500\times$. A similar enhancement characterizes ^{15}N sites in the NH_3 region as well as arginine's guanidine ^{15}N sites in the lysate. The only amide nitrogens that do not appear enhanced are those belonging to proline groups, owing to their lack of exchangeable protons.

4. DISCUSSION AND CONCLUSIONS

Bringing the benefits of DNP to bear onto the study of biomolecules in solution is an important challenge in contemporary NMR. The present work investigated a way of bypassing the T_1 bottleneck that slowly tumbling biomacro-

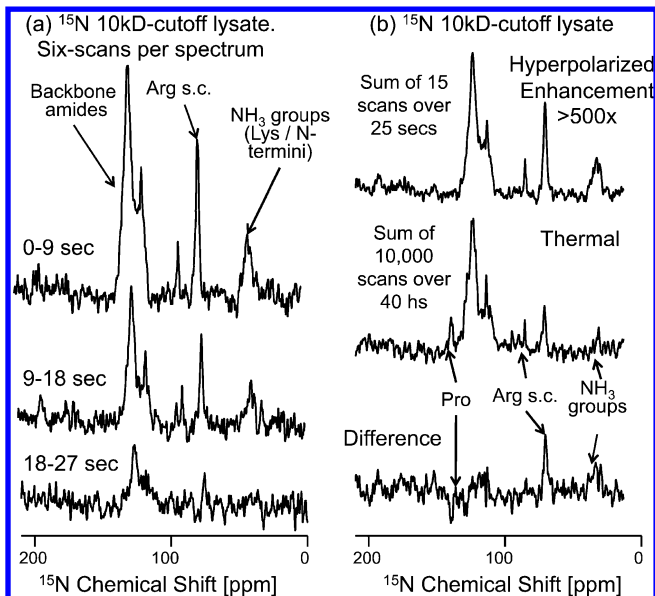


Figure 7. Enhancement of ¹⁵N signals in a ¹⁵N-labeled polypeptide lysate with molecular weight cutoff of 10 kDa via polarization transfer from hyperpolarized water. (a) ¹⁵N NMR spectra arising from 90° ¹⁵N pulses applied over the indicated postdissolution times, reflecting the 17.9 s T_1 we detect for the water protons onto the ¹⁵N signals enhanced by the exchangeable protons. The sum of six consecutive scans from this time series is displayed. (b) Sum of first 15 scans (upper trace) following the injection of hyperpolarized water compared versus a thermal equilibrium ¹⁵N spectrum (middle trace), measured by signal-averaging 10 000 scans over the course of ca. 40 h. The difference between these spectra is displayed in the bottom trace, highlighting the over-enhancement of the arginine side chains (NH₂) and lysine's (NH₃) groups and the under-enhancement of the protonless proline backbone nitrogens. The average signal enhancement of the ¹⁵N backbone amides is >500× relative to ¹⁵N thermal equilibrium signal. Other acquisition parameters are as in Figure 5

molecules will face upon transferring from the DNP to the NMR fields, based on an *ex situ* hyperpolarization of water and subsequent exchange-driven transfers of polarization to labile biomolecular sites. Although addressing a small subset of all sites, such an efficient enhancement of exchangeable protons, and of their bonded nitrogens, could facilitate a wide variety of studies currently supported, *inter alia*, by ¹H-¹⁵N 2D correlations. This strategy's success depends on maximizing the absolute polarization of the H₂O achieved in the cryogenic solid, minimizing the dilution that the cryogenic pellet will undergo upon melting and shuttling, and reducing the ¹H relaxation losses that limit the time over which the H₂O polarization can be exploited in the biomolecular analyses. The present study placed an emphasis on optimizing the last two of these aspects, with dilution and relaxation losses minimized by a combination of dissolution and transfer precautions. With these provisions dilution penalties were limited to ~90%, a non-negligible factor that is still liable to improvement, and relaxation times reached 15–20 s. All of this translated into ~100× enhancements over the polarization characterizing a tube of pure water placed in a high field system. Even further room for enhancement remains in terms of optimizing the cryogenic solid-state polarization, as witnessed by the fact that electrons are over 90% polarized in the DNP setup used whereas the ¹H polarization hardly cleared the 5% mark.

Even with these limitations, an interesting aspect of the examined approach lies in its ability to spontaneously enhance the resonances of ¹⁵N attached to labile protons by factors in the 100–1000× range. These results are particularly promising for ¹⁵N sites that undergo rapid ¹H exchange, for example, lysine side chains and amide positions in unstructured proteins at high pH; these sites cannot be efficiently enhanced by INEPT-like sequences, while thermal equilibrium ¹H→¹⁵N NOE methods are inefficient in macromolecules. The spontaneous nature of the transfer is also promising for human-oriented NMR imaging setups, which are rarely equipped with full double-resonance irradiation capabilities. It is conceivable, however, that a more active INEPT-like transfer might be more effective for N–H sites undergoing intermediate proton exchange than the spontaneous transfer assayed in this study. We have carried out such tests, but preliminary results indicate that this strategy is challenged if attempting to leave the radiation-broadened reservoir of hyperpolarized H₂O untouched for the sake of performing multiple ¹⁵N acquisitions. Further efforts aimed at clarifying these issues are ongoing.

The enhanced biomolecular sensitivity experiments demonstrated in this work were carried out on intrinsically unfolded systems liable to fast hydrogen exchange of their backbone protons. Additional potential targets could include structured polypeptides that are kept artificially unfolded in the NMR tube where their measurement will take place, until the arrival of hyperpolarized water triggers their sudden folding. Even in folded systems, sensitivity gains should arise from water-accessible side chains whose protons are rapidly exchanging with those of the hyperpolarized water. A different kind of experimental window that might be opened by the hyperpolarized experiments hereby described, involves measuring the rates of water exchange or water accessibility in biomolecules.³⁸ Two kinds of water–proton exchange experiments are commonly used, depending on the range of exchange rates to be accessed. Slower exchange processes are usually determined by isotope dilution methods, whereby the volumes of proton peaks in proteins whose exchangeable sites were fully deuterated are monitored in real time as the sample is diluted by fully protonated water (or conversely, whereby peak decays are quantified as a fully protonated protein is diluted in deuterated water).^{39,40} Another method, better suited for studying more rapid exchange processes, relies on observing the decrease in the intensities of the labile peaks upon solvent water saturation/inversion. In this method, the signal of the individual exchangeable proton sites will depend on k_{ex} as well as on the site's T_1 value, and hence these experiments are limited to k_{ex} on the order of the site's T_1 (*i.e.*, $k_{\text{ex}} \approx 1 \text{ s}^{-1}$).⁴¹ Studying hydrogen exchange processes using the hyperpolarized water principles described in this paper has many features that complement both of these methods, both due to its real-time nature and by virtue of the various time scales that the hyperpolarization lifetime enables one to probe. In particular, the fact that a high signal contrast is not governed solely by the intrinsic T_1 of the exchanging sites but rather by $T_1(\text{H}_2\text{O})$ (Figure 3C, bottom) means that it should be possible to characterize slower rates of k_{ex} than in conventional magnetization transfer methods. This research avenue is currently being investigated.

■ ASSOCIATED CONTENT

● Supporting Information

Summary of dilution factors, postdissolution polarizations, and experimental T_1 values observed for different volume and dissolution conditions. Modeling of the heteronuclear signal enhancement spontaneously derived from hyperpolarized H_2O injections. This material is available free of charge via the Internet at <http://pubs.acs.org>.

■ AUTHOR INFORMATION

Corresponding Author

*E-mail: lucio.frydman@weizmann.ac.il. Tel: +972-8-934-4903.

Notes

The authors declare no competing financial interest.

■ ACKNOWLEDGMENTS

We are grateful to K. Zibzener for assistance with the experiments and to Dr. Shira Albeck (ISPC, Weizmann Institute) for the preparation of the reductase lysate. Financial support from ERC Advanced Grant #246754, EU's BioNMR Grant #261863, DIP Project 710907 (Ministry of Education and Research, Germany), the Clore Foundation and the generosity of the Perlman Family Foundation, are also acknowledged.

■ REFERENCES

- (1) Abragam, A.; Goldman, M. Principles of Dynamic Nuclear Polarisation. *Rep. Prog. Phys.* **1978**, *41* (3), 395.
- (2) Wind, R. A. Dynamic Nuclear Polarization and High-Resolution NMR of Solids. In *eMagRes*; John Wiley & Sons, Ltd: New York, 2007.
- (3) Barnes, A. B.; De Paëpe, G.; van der Wel, P. C. A.; Hu, K. N.; Joo, C. G.; Bajaj, V. S.; Mak-Jurkauskas, M. L.; Sirigiri, J. R.; Herzfeld, J.; Temkin, R. J.; et al. High-Field Dynamic Nuclear Polarization for Solid and Solution Biological NMR. *Appl. Magn. Reson.* **2008**, *34* (3–4), 237–263.
- (4) Maly, T.; Debelouchina, G. T.; Bajaj, V. S.; Hu, K.-N.; Joo, C.-G.; Mak-Jurkauskas, M. L.; Sirigiri, J. R.; Wel, P. C. A. v. d.; Herzfeld, J.; Temkin, R. J.; et al. Dynamic Nuclear Polarization at High Magnetic Fields. *J. Chem. Phys.* **2008**, *128* (5), 052211.
- (5) Prisner, T.; Köckenberger, W. Dynamic Nuclear Polarization: New Experimental and Methodology Approaches and Applications in Physics, Chemistry, Biology and Medicine. *Appl. Magn. Reson.* **2008**, *34* (3–4), 213–218.
- (6) Griffin, R. G.; Prisner, T. F. High Field Dynamic Nuclear Polarization—the Renaissance. *Phys. Chem. Chem. Phys.* **2010**, *12* (22), 5737–5740.
- (7) Bennati, M.; Tkach, I.; Turke, M. T., Dynamic Nuclear Polarization in Liquids. In *Electron Paramagnetic Resonance*; The Royal Society of Chemistry: Oxford, U.K., 2011; Vol. 22, pp 155–182.
- (8) Rossini, A. J.; Zagdoun, A.; Hegner, F.; Schwarzwälder, M.; Gajan, D.; Copéret, C.; Lesage, A.; Emsley, L. Dynamic Nuclear Polarization NMR Spectroscopy of Microcrystalline Solids. *J. Am. Chem. Soc.* **2012**, *134* (40), 16899–16908.
- (9) Ardenkjær-Larsen, J. H.; Fridlund, B.; Gram, A.; Hansson, G.; Hansson, L.; Lerche, M. H.; Servin, R.; Thaning, M.; Golman, K. Increase in Signal-to-Noise Ratio of > 10,000 Times in Liquid-State NMR. *Proc. Natl. Acad. Sci. U. S. A.* **2003**, *100* (18), 10158–10163.
- (10) Kurhanewicz, J.; Vigneron, D. B.; Brindle, K.; Chekmenev, E. Y.; Comment, A.; Cunningham, C. H.; DeBerardinis, R. J.; Green, G. G.; Leach, M. O.; Rajan, S. S.; et al. Analysis of Cancer Metabolism by Imaging Hyperpolarized Nuclei: Prospects for Translation to Clinical Research. *Neoplasia* **2011**, *13* (2), 81–97.
- (11) Wolber, J.; Ellner, F.; Fridlund, B.; Gram, A.; Jóhannesson, H.; Hansson, G.; Hansson, L. H.; Lerche, M. H.; Måansson, S.; Servin, R.; et al. Generating Highly Polarized Nuclear Spins in Solution Using Dynamic Nuclear Polarization. *Nucl. Instrum. Methods Phys. Res., Sect. A* **2004**, *526* (1–2), 173–181.
- (12) Day, S. E.; Kettunen, M. I.; Gallagher, F. A.; Hu, D. E.; Lerche, M.; Wolber, J.; Golman, K.; Ardenkjær-Larsen, J. H.; Brindle, K. M. Detecting Tumor Response to Treatment Using Hyperpolarized C-13 Magnetic Resonance Imaging and Spectroscopy. *Nat. Med.* **2007**, *13* (11), 1382–1387.
- (13) Mieville, P.; Jannin, S.; Helm, L.; Bodenhausen, G. NMR of Insensitive Nuclei Enhanced by Dynamic Nuclear Polarization. *Chimia* **2011**, *65* (4), 260–263.
- (14) Bornet, A.; Melzi, R.; Jannin, S.; Bodenhausen, G. Cross Polarization for Dissolution Dynamic Nuclear Polarization Experiments at Readily Accessible Temperatures $1.2 < t < 4.2$ K. *Appl. Magn. Reson.* **2012**, *43* (1–2), 107–117.
- (15) Bornet, A.; Melzi, R.; Perez Linde, A. J.; Hautle, P.; van den Brandt, B.; Jannin, S.; Bodenhausen, G. Boosting Dissolution Dynamic Nuclear Polarization by Cross Polarization. *J. Chem. Phys. Lett.* **2012**, *4* (1), 111–114.
- (16) Hurd, R. E.; Yen, Y.-F.; Chen, A.; Ardenkjær-Larsen, J. H. Hyperpolarized ^{13}C Metabolic Imaging Using Dissolution Dynamic Nuclear Polarization. *J. Magn. Reson. Imaging* **2012**, *36* (6), 1314–1328.
- (17) Jannin, S.; Bornet, A.; Melzi, R.; Bodenhausen, G. High Field Dynamic Nuclear Polarization at 6.7 T: Carbon-13 Polarization above 70% within 20 min. *Chem. Phys. Lett.* **2012**, *549* (0), 99–102.
- (18) Mishkovsky, M.; Eliav, U.; Navon, G.; Frydman, L. Nearly 10^6 -Fold Enhancements in Intermolecular ^1H Double-Quantum NMR Experiments by Nuclear Hyperpolarization. *J. Magn. Reson.* **2009**, *200* (1), 142–146.
- (19) Lerche, M. H.; Meier, S.; Jensen, P. R.; Hustvedt, S.-O.; Karlsson, M.; Duus, J. Ø.; Ardenkjær-Larsen, J. H. Quantitative Dynamic Nuclear Polarization-NMR on Blood Plasma for Assays of Drug Metabolism. *NMR Biomed.* **2011**, *24* (1), 96–103.
- (20) Ragavan, M.; Chen, H.-Y.; Sekar, G.; Hilty, C. Solution NMR of Polypeptides Hyperpolarized by Dynamic Nuclear Polarization. *Anal. Chem.* **2011**, *83* (15), 6054–6059.
- (21) Kay, L. E.; Torchia, D. A.; Bax, A. Backbone Dynamics of Proteins as Studied by ^{15}N Inverse Detected Heteronuclear NMR Spectroscopy: Application to Staphylococcal Nuclease. *Biochemistry* **1989**, *28* (23), 8972–8979.
- (22) Yao, S.; Babon, J. J.; Norton, R. S. Protein Effective Rotational Correlation Times from Translational Self-Diffusion Coefficients Measured by PFG-NMR. *Biophys. Chem.* **2008**, *136* (2–3), 145–151.
- (23) Ferrage, F.; Dutta, K.; Shekhtman, A.; Cowburn, D. Structural Determination of Biomolecular Interfaces by Nuclear Magnetic Resonance of Proteins with Reduced Proton Density. *J. Biomol. NMR* **2010**, *47* (1), 41–54.
- (24) Leggett, J.; Hunter, R.; Granwehr, J.; Panek, R.; Perez-Linde, A. J.; Horsewill, A. J.; McMaster, J.; Smith, G.; Kockenberger, W. A Dedicated Spectrometer for Dissolution DNP NMR Spectroscopy. *Phys. Chem. Chem. Phys.* **2010**, *12* (22), 5883–5892.
- (25) Bowen, S.; Hilty, C. Time-Resolved Dynamic Nuclear Polarization Enhanced NMR Spectroscopy. *Angew. Chem., Int. Ed.* **2008**, *47* (28), 5235–5237.
- (26) Bowen, S.; Hilty, C. Rapid Sample Injection for Hyperpolarized NMR Spectroscopy. *Phys. Chem. Chem. Phys.* **2010**, *12* (22), 5766–5770.
- (27) Barb, A. W.; Hekmatyar, S. K.; Glushka, J. N.; Prestegard, J. H. Exchange Facilitated Indirect Detection of Hyperpolarized $^{15}\text{ND}_2$ -Amido-Glutamine. *J. Magn. Reson.* **2011**, *212* (2), 304–310.
- (28) Massiot, D.; Fayon, F.; Capron, M.; King, I.; Le Calvé, S.; Alonso, B.; Durand, J.-O.; Bujoli, B.; Gan, Z.; Hoatson, G. Modelling One- and Two-Dimensional Solid-State NMR Spectra. *Magn. Reson. Chem.* **2002**, *40* (1), 70–76.
- (29) Ardenkjær-Larsen, J. H.; Laustsen, C.; Pullinger, B.; Kadlec, S.; Emami, K.; Rizi, R. Hyperpolarized Water for Interventional Angiography. *Proc. Int. Soc. Mag. Reson. Med.* **2011**, *19*, 3534.

(30) Harris, T.; Bretschneider, C.; Frydman, L. Dissolution DNP NMR with Solvent Mixtures: Substrate Concentration and Radical Extraction. *J. Magn. Reson.* **2011**, *211* (1), 96–100.

(31) Polnaszek, C. F.; Bryant, R. G. Nitroxide Radical Induced Solvent Proton Relaxation: Measurement of Localized Translational Diffusion. *J. Chem. Phys.* **1984**, *81* (9), 4038–4045.

(32) Bennati, M.; Luchinat, C.; Parigi, G.; Turke, M.-T. Water ^1H Relaxation Dispersion Analysis on a Nitroxide Radical Provides Information on the Maximal Signal Enhancement in Overhauser Dynamic Nuclear Polarization Experiments. *Phys. Chem. Chem. Phys.* **2010**, *12* (22), 5902–5910.

(33) McCarney, E. R.; Armstrong, B. D.; Lingwood, M. D.; Han, S. Hyperpolarized Water as an Authentic Magnetic Resonance Imaging Contrast Agent. *Proc. Natl. Acad. Sci. U. S. A.* **2007**, *104* (6), 1754–1759.

(34) McConnell, H. M. Reaction Rates by Nuclear Magnetic Resonance. *J. Chem. Phys.* **1958**, *28* (3), 430–431.

(35) Henry, G. D.; Sykes, B. D. Determination of the Rotational Dynamics and pH Dependence of the Hydrogen Exchange Rates of the Arginine Guanidino Group Using NMR Spectroscopy. *J. Biomol. NMR* **1995**, *6* (1), 59–66.

(36) Liepinsh, E.; Otting, G. Proton Exchange Rates from Amino Acid Side Chains—Implications for Image Contrast. *Magn. Reson. Med.* **1996**, *35* (1), 30–42.

(37) Krishna, N. R.; Goldstein, G.; Glickson, J. D. A General Multistate Model for the Analysis of Hydrogen-Exchange Kinetics. *Biopolymers* **1980**, *19* (11), 2003–2020.

(38) Armstrong, B. D.; Han, S. Overhauser Dynamic Nuclear Polarization to Study Local Water Dynamics. *J. Am. Chem. Soc.* **2009**, *131* (13), 4641–4647.

(39) Englander, S. W.; Mayne, L. Protein Folding Studied Using Hydrogen-Exchange Labeling and Two-Dimensional NMR. *Annu. Rev. Biophys. Biomol. Struct.* **1992**, *21* (1), 243–265.

(40) Englander, S. W. Protein Folding Intermediates and Pathways Studied by Hydrogen Exchange. *Annu. Rev. Biophys. Biomol. Struct.* **2000**, *29* (1), 213–238.

(41) Waelder, S.; Lee, L.; Redfield, A. G. Nuclear Magnetic Resonance Studies of Exchangeable Protons. I. Fourier Transform Saturation-Recovery and Transfer of Saturation of the Tryptophan Indole Nitrogen Proton. *J. Am. Chem. Soc.* **1975**, *97* (10), 2927–2928.